COBEM 2021 26th International Congress of Mechanical Engineering
November 22-26, 2021, Virtual Congress, Brazil

COB-2021-1892
NUMERICAL ANALYSIS OF CONDUCTION AND THERMAL CONTACT RESISTANCE IN MULTI-LAYERED CUTTING TOOL

Rafael Thomaz de Camargo Rodrigues
Institute of Integrated Engineering - IEI. Federal University of Itajubá - UNIFEI, Itabira, MG, Brazil.
rafa.rodrigues13.rr@gmail.com

Paulo Mohallem Guimarães
Institute of Integrated Engineering - IEI. Federal University of Itajubá - UNIFEI, Itabira, MG, Brazil.
pauloguimaraes@unifei.edu.br

Júlio Cesar Costa Campos
Postgraduate Program in Energy Engineering - Federal University of São João Del Rei - UFSJ. Thermal Systems Laboratory, Department of Mechanical Engineering, Federal University of Viçosa - UFV, Viçosa, MG, Brazil.
julio.campos@ufv.br

Sandro Metrevelle Marcondes de Lima e Silva
Institute of Mechanical Engineering. Federal University of Itajubá, Campus Professor José Rodrigues Seabra, Avenida BPS 1303, 37500-903 Itajubá, MG, Brazil.
metrevel@unifei.edu.br

José Carlos de Lacerda
Institute of Integrated Engineering - IEI. Federal University of Itajubá - UNIFEI, Itabira, MG, Brazil.
jlacerda@unifei.edu.br

Rogério Fernandes Brito
Institute of Integrated Engineering - IEI. Federal University of Itajubá - UNIFEI, Itabira, MG, Brazil.
rogbrito@unifei.edu.br

Abstract. *Through the process of turning, the cutting tool is heated during its use. Temperatures can reach values above 900ºC. Upon reaching these temperature levels, the cutting tool loses its mechanical properties and wears out prematurely. To alleviate this problem, one of the solutions found was to coat the cutting tools with a thin layer of material with thermal insulating characteristics. Thus, the purpose of this work was to numerically simulate the phenomenon of heating, in transient regime, a tool and tool holder set while considering the presence of the coating as well as to evaluate the heat exchange by conduction. Another factor considered in this work was the presence of the contact resistance between the tool and the tool holder, which, according to some studies, has an impact on the temperature field of the cutting tool. In this research, the thermophysical properties of the elements under analysis are treated as temperature dependent. Some parameters related to the contact resistance are taken into account to make the model closer to real situations. Simulations were carried out using the COMSOL® program to solve the transient three-dimensional heat diffusion equation using the Finite Element Method. After that, the temperatures found for the uncoated cutting tool (substrate only) were compared to the temperatures found for the case of the cutting tool coated with Titanium Nitride (TiN), Aluminum Oxide (Al_2O_3), and Titanium Carbide (TiC).*

Keywords: *Cutting Tool, Heat Transfer, COMSOL®, Coating, Contact Resistance.*

1. INTRODUCTION

The machining process, like other processes that perform high material deformations, generates a large amount of heat. Heat is a parameter that has a strong influence on the tool's performance throughout this process. In light of this, the importance of developing new materials resistant to high temperatures and methods of prolonging the life of cutting tools is evident, thus allowing for high cutting speeds in machining processes and reducing the replacement costs of such tools.

Determining the temperature during cutting is one of the most important factors in the study of tool performance as it allows for the analysis and understanding of the factors that influence its ultimate wear and life (Borelli *et al.*, 2001). Furthermore, there is currently a sharp reduction in the use of lubricants and refrigerants due to their impact on the

environment and their influence on the increase in machining costs, corroborating the need for further studies in this thermal area (Tonshoff *et al.*, 2000 and Yen *et al.*, 2004).

Another way to increase tool life is to coat the tool's cutting surface with materials with thermal insulation characteristics that provide less wear on the tool. Coatings for cutting tools emerged for the purpose of associating wear resistance and toughness. New coating materials have since been developed and the improvement in performance can be credited to their thermal characteristics. Therefore, it is important to investigate the thermal influence of these coatings on cutting tools. According to Hunt and Santhanam (1990), productivity reached levels two to three times higher when compared to uncoated tools in the turning process.

Therefore, this work proposes the study of the thermal influence of these coatings on cemented carbide cutting tools. For this reason, the coating is modeled as a thin layer positioned on top of the cutting tool in a three-dimensional numerical model. With defined boundary conditions and known heat flux from existing literature-based data, the temperature field in the cutting tool can be determined.

1.1 Numerical Studies of Heat Transfer

Extensive work has been done to find these solutions. Song *et al.* (2017) analyzed the variation of the cutting temperature in machining with a cemented carbide tool in two cases, one with the tool coated with Ti-MoS_2/Zr composite and the other using the tool without coating.

Using a different composite for the coating, TiAlN/AlCrN, Ghani *et al.* (2016) studied the wear process that occurs in the cutting tool, analyzing the cases of coated and uncoated tools.

The use of coatings remains the most efficient solution, according to Grzesik (2006). In his work, three composites that have good characteristics and applicability for cutting tool coatings were considered, namely Titanium Nitride (TiN), Titanium Carbide (TiC), and Alumina Oxide (Al_2O_3). Furthermore, several works treat these coatings with these composites.

Zhang and Liu (2017) analyzed the temperature distribution in steady state and transient in cemented carbide cutting tools with a coating layer, such as TiN, TiC and Al_2O_3. According to the results obtained, the tool with Al_2O_3 composite coating is the most effective in reducing heat conduction during the machining process.

A study conducted by Zhang *et al.* (2017) showed a new prediction model that predicts the temperature distribution on the cutting face of a tool with a coating layer based on heat source theory. Based on their the analysis, the authors concluded that the two coated tools generated lower temperatures on the tool's cutting face when compared to the uncoated tool, thus proving that the coating is efficient in prolonging tool life.

In the work by Jin *et al.* (2018) the heat partition model for a cutting tool was developed using the finite element method to study the heat conduction mechanism in the secondary strain zone. Throughout the research, the authors carried out cutting experiments with tools coated with four different types of materials, most notably TiC, TiN, TiAlN, and Al_2O_3. A comparison of the temperatures obtained on the cut face for each type of coating was performed.

Ferreira *et al.* (2018) used the numerical analysis of the influence of coatings on a cutting tool using the *COMSOL*® software and an inverse nonlinear problem. For the study, TiN and Al_2O_3 were used as the coating materials. The research was carried out using numerical methods since experimental methods have their limitations for determining the temperature on the tool surface. The heat flux was estimated using *COMSOL*® and was later compared with previous work by Brito *et al.* (2009). Ferreira *et al.* (2018) concluded that the best results were with the Al_2O_3 coating.

Hao and Liu (2019) performed dry cut tests with H13 hardened steel using a TiAlN composite coating, including Thermal Contact Resistance (TCR) among the parts of the assembly.

Thus, we used computational tools in CAD and CAE in the present work, in which the heat flux adopted was obtained from Carvalho *et al.* (2006). Nonlinear thermal properties were defined and determined from adjustment equations as a function of temperature as described by Incropera *et al.* (2011). The temperature-dependent thermophysical properties adopted in the models, with the exception of the emissivity and the temperature-dependent thermal property values of 1045 steel, the tool holder material, were obtained from Grzesik, *et al.* (2009). Cemented carbide tool emissivity values varying with temperature were obtained from the work of Jiang *et al.* (2016).

Figure 1 shows the unstructured finite element mesh in the contact area at the typical chip-tool interface used in the numerical simulations of the present work with an area of approximate value of 1.424 mm^2. This area was obtained experimentally by Carvalho *et al.* (2006).

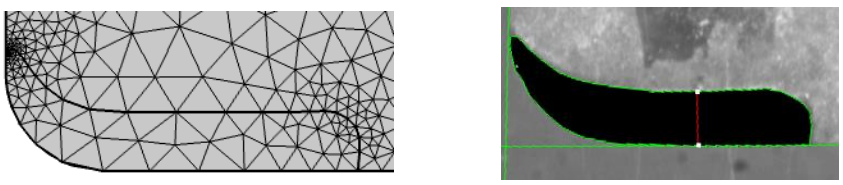

(a) (b)

Figure 1. Unstructured finite element mesh of the tool of this work, being (a) a partial detail of the heat flux region and (b) a video image of the contact area at the chip-workpiece-tool interface (Carvalho *et al.*, 2006).

To model the natural convection heat transfer coefficient varying with temperature, the *COMSOL*® software uses the empirical correlations of Incropera *et al.* (2011). For the numerical validation of the present work, an average value of the convective heat transfer coefficient equal to 20 W/m²K was chosen, according to Carvalho *et al.* (2006). Furthermore, in the present work, the TCR between the parts of the tool was implemented based on experimental data from Corrêa Ribeiro (2018) and is available in the *COMSOL*® package. As such, it was necessary to obtain the following parameters: the inclusion of the micro hardness of the tool, the cutting force, and the clamping force of the clamp, which holds the cutting tool together, considering only one coating material.

2. METHODOLOGY

Thus, the present work, in addition to the implementation of TCR and the natural convection coefficient, presented an improvement in relation to previous works by the present authors, considering the numerical simulation with multiple coating layers on the tool in order to seek a more realistic model.

2.1 Problem description

The numerical thermal model used in this work was a carbide cutting tool, tool holder, and a shim, based on the experimental and numerical work of Carvalho *et al.* (2006). Two analyses were carried out. In the first analysis, only the uncoated cemented carbide tool was considered, and in the second analysis the tool having multi-layer coating was considered. From these two models, numerical simulations were carried out to analyze the effect of the coating on the temperature field that forms on the tool during the machining process. Shown below are the main dimensions in mm of the substrate of the cemented carbide cutting tool (Figure 2a), the tool holder (Figure 2b), and the shim (Figure 2c) used in the models.

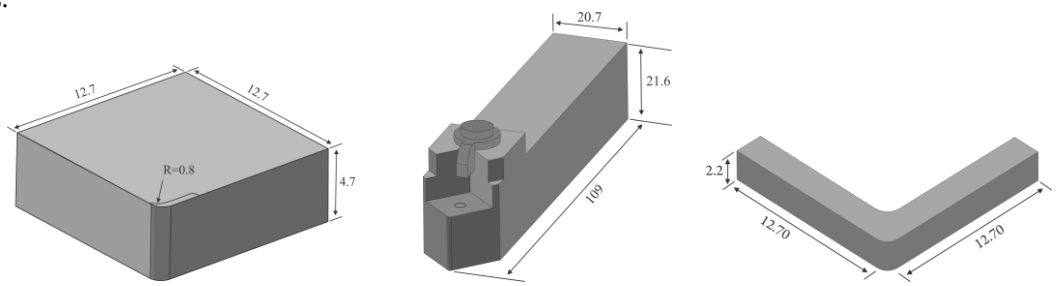

(a) (b) (c)

Figure 2. Main dimensions (mm): (a) cemented carbide cutting tool, (b) tool holder, and (c) shim.

Below, Figure 3a shows a portion of the coating detailing the contact area between the cutting tool and the part, which is represented in yellow in this figure. In order to facilitate the illustration and differences between the two models studied, both models were divided into domains: cemented carbide cutting tool substrate (Ω_1), shim (Ω_2), tool holder (Ω_3), TiC coating (Ω_4), Al_2O_3 coating (Ω_5), and TiN coating (Ω_6) (GRZESIK, 2006).

The contact region between the cutting tool and the part, which is shown in Figure 3a in yellow color, was modeled considering the experimental measurement made by Carvalho *et al.* (2006) through the use of an image analyzer. In Figures 3b and 3c, the region measured experimentally (Fig. 3b) is compared with the region S_1 of the numerical model (Fig. 3c) of the present work.

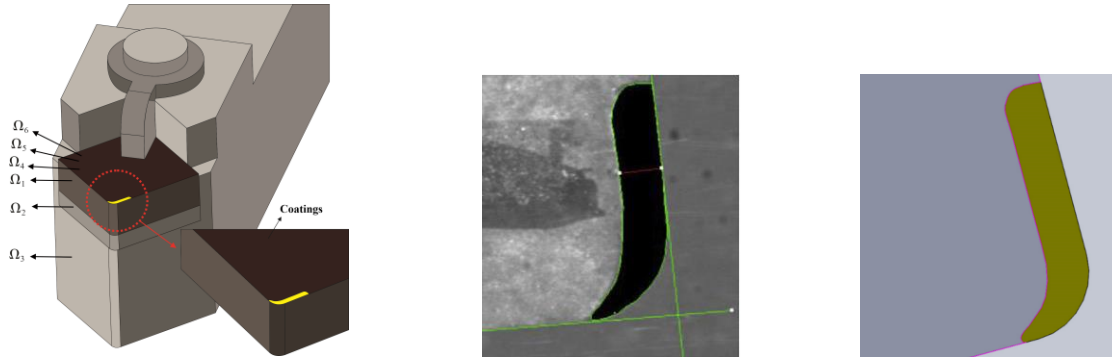

(a) (b) (c)

Figure 3. (a) Assembly of the tool and tool holder set and detail of the coatings. Comparison between the contact areas of the cutting tool: (b) experimental and (c) numerical in this work.

The temperature-dependent thermophysical properties adopted in the present work, with the exception of emissivity, and the temperature-dependent thermal tool holder material property values of 1045 steel were taken from the work of Grzesik *et al.* (2009). Cemented carbide tool emissivity values varying with temperature were obtained from the work of Jiang *et al.* (2016).

In this work, the presence of thermal radiation is also considered in the simulation of the models, making it necessary to know the emissivity values of the materials. Numerical data obtained from the convective heat transfer coefficient of Carvalho *et al.* (2006) and Incropera *et al.* (2011) were used. Cemented carbide tool emissivity values, considering temperature variation, were obtained from the work by Jiang *et al.* (2016).

The emissivity of TiN, Al_2O_3, and 1045 steel was taken from the studies by Yuste *et al.* (2010), Wang *et al.* (2013), and Polozine and Schaeffer (2005), and their values were respectively equal to: 0.2; 0.85, and 0.83. In the case of TiC emissivity, 0.2 was adopted in the present work.

Some hypotheses were adopted in the two proposed models, such as perfect thermal contact between the coating and the substrate; emissivity of constant materials, in relation to temperature, for the coating and tool holder; and constant ambient temperature and absence of internal heat generation in all domains that were studied.

The resolution of the thermal problem presented in this work was done using the direct method in order to obtain the value of numerical temperatures since all boundary conditions were already known. The governing equations of the studied physical problem are shown below.

2.2 Thermal Model

The equation that describes the thermal model used is the transient three-dimensional heat diffusion equation (Eq. 1), considering variable properties with temperature:

$$\frac{\partial}{\partial x}k(T)\frac{\partial T}{\partial x}(x,y,z,t)+\frac{\partial}{\partial y}k(T)\frac{\partial T}{\partial y}(x,y,z,t)+\frac{\partial}{\partial z}k(T)\frac{\partial T}{\partial z}(x,y,z,t)=\rho c_p(T)\frac{\partial T}{\partial t}(x,y,z,t). \quad (1)$$

Subject to the convection and radiation boundary condition (Eq. 2):

$$-k(T)\frac{\partial T}{\partial \eta}(x,y,z,t)=h(T)(T-T_\infty)+\sigma\varepsilon(T)(T^4-T_\infty^4). \quad (2)$$

In the area of contact between the tool and the workpiece, the boundary condition is imposed transient heat flux (Eq. 3):

$$-k(T)\frac{\partial T}{\partial z}(x,y,0,t)=\ q_0^{"}(t) \text{ em } S_1. \quad (3)$$

The initial condition of the model used for all domains is given by Eq. 4:

$$T(x,y,z,0)=\ T_0. \quad (4)$$

2.3 Numerical method

All numerical simulations in this work were performed with the commercial program *COMSOL*® Multiphysics 5.4, which uses the finite element method. In the case of heat transfer problems in transient solids, *COMSOL*® uses the BDF (backward differentiation formula) method to approximate the time derivatives and the GMRES (generalized minimum residual) method, being an iterative method for the resolution of general linear systems in the formula Ax = b.

In the case of modeling the natural convection coefficient varying with temperature, *COMSOL*® uses the empirical correlations of Incropera *et al.* (2011) that are already implemented in this computational package.

On all surfaces, air was considered as the surface contact fluid with an external ambient temperature of 29.2°C and an absolute pressure of 1 atm.

2.4 Experimental Procedure

One of the main difficulties in analyzing a machining process through a thermal look is knowing the precise heat flow at the contact interface between the part and the cutting tool. For that to happen, it is necessary to carry out experimental tests to obtain the thermal field in the set. The present work used experimental and numerical temperature and transient heat flux data from Carvalho *et al.* (2006). This heat flux is used in the present work as a boundary condition applied in

area S_1 (Figure 3c). Figure 4 shows the positions of the sensors, which are used by Carvalho *et al.* (2006), in order to obtain the temperature field and verify the thermal influence of multilayer coatings.

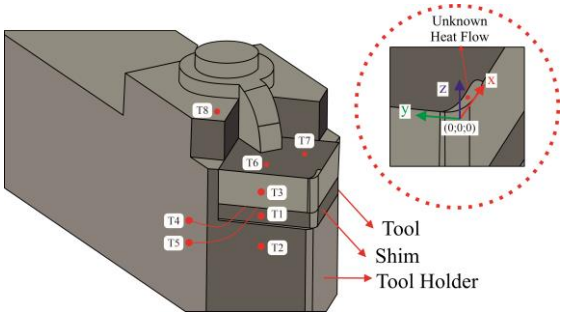

Figure 4. Positioning thermocouples T1 to T8 in the tool set, shim, and tool holder.

The cutting parameters used in this work were the following: 0.138 mm feed/revolution; cutting speed of 135.47 m/min; initial diameter of 77.0 mm; machined length of 77.0 mm; 5.0 mm cutting depth and 580.0 rpm rotation (CARVALHO *et al.*, 2006).

2.5 Thermal Contact Resistance (TCR)

In composite systems with two or more materials or parts, there may be an abrupt drop in temperature at the interface between the materials due to imperfect contact between them (Incropera *et al.*, 2011).

In the present work, the analysis of the thermal contact resistance (TCR) was considered based on data obtained from Corrêa Ribeiro (2018). The TCR is extensively present in any assembly and modifies the heat conduction pattern as it occurs in electronic circuits, among other equipment (Corrêa Ribeiro, 2018).

In order for the *COMSOL*® software to calculate the contact resistance, it was necessary to collect the data used as parameters between any two domains from the literature, namely: the convective heat transfer coefficient present in the air-filled interstices, h_g; mean surface roughness, σ_{asp}; slope of roughness peaks, m_{asp}; softer surface hardness, H_c; and contact pressure, P. In this work, the values adopted for the required parameters were taken from the work of Corrêa Ribeiro (2018).

2.6 Obtaining Temperature Profiles

In addition to the use of thermocouples for the analysis of temperature at various points on the tool and the tool holder, in this work numerical probes were additionally inserted along the cutting tool and positioned according to the coordinates indicated in Table 1 in both cases analyzed.

The probes are evenly distributed over the first 10 µm, which is the thickness of the coating adopted. Next, a schematic drawing is presented in Figure 5 to better explain the placement of the numerical probes along the set.

Table 1. Coordinates of numerical probes.

Probe	R00	R01	R02	R03	R04	R05	R06	R07	R08	R09	R10
x [mm]	0.25	0.25	0.25	0.25	0.25	0.25	0.25	0.25	0.25	0.25	0.25
y [mm]	1.35	1.35	1.35	1.35	1.35	1.35	1.35	1.35	1.35	1.35	1.35
z [mm]	0.000	-0.001	-0.002	-0.003	-0.004	-0.005	-0.006	-0.007	-0.008	-0.009	-0.010

In Figure 5, the R00 probe was positioned in order to calculate the temperatures on the tool exit surface, that is, in the region that would be the interface between the chip and the cutting tool in a real model. The R10 probe is located 10 µm below the exit surface, being the point equivalent to the interface between the coatings and the substrate in the cases that consider the coatings. This distribution is adopted in both cases with and without coating in order to investigate the thermal influence of different thermal properties and different materials.

3. RESULT ANALYSIS

3.1 Numeric Model Validation

To validate the numerical methodology implemented in this work, numerical simulations of the thermal influence of the mesh refinement were performed, using the commercial package *COMSOL*® Multiphysics 5.4. In this numerical analysis, experimental data from Carvalho *et al.* (2006), considering an ISO K10 cemented carbide cutting tool with dimensions 12.7 mm x 12.7 mm x 4.7 mm with thermophysical properties (Fig. 6): k = 43.1 W m^{-1} K^{-1}, c_p = 332.94 J kg^{-1} K^{-1} e ρ = 14,900.00 kg m^{-3}.

Source: Adapted from Corrêa Ribeiro (2018).

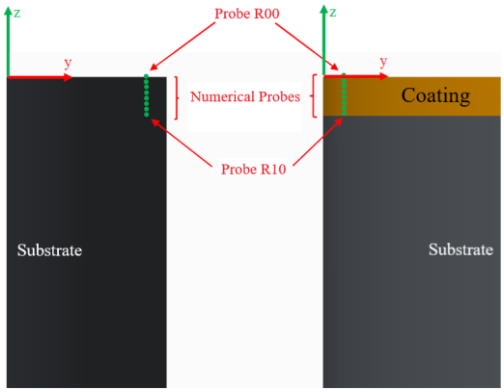

(a) (b)

Figure 5. Positioning, without scaling, of the numerical probes in the uncoated (a) and coated (b) model. Source: adapted from Corrêa Ribeiro (2018).

In his laboratory-controlled experiment, Carvalho *et al.* (2006) placed a resistive heater, a heat flux transducer, and two thermocouples on the cutting tool in which all sensors were previously calibrated. The author connected the resistive heater to a direct current source that, by the Joule effect, provided the heat generation. He also positioned the heat flux transducer between the heater and the tool in order to measure the thermal flux supplied to the cutting tool. Cutting tool temperatures were measured from two thermocouples connected to a computer-controlled Agilent 34980A data acquisition system.

In the isolated cutting tool (Figure 6), there are two thermocouples for calculating the temperature: thermocouple 1 at point x = 3.5 mm, y = 8.9 mm, and z = 4.7 mm; and thermocouple 2 at point x = 6.5 mm, y = 5.9 mm, and z = 4.7 mm.

In the present work, three computational meshes were generated to carry out the study of the independence of the mesh on the obtained temperature results, namely the mesh entitled "coarser," "normal," and "finer," which are refinements pre-defined in the software of *COMSOL*® simulation. Tables 2 and 3 show the results of the deviations with variations in the number of elements, number of nodes, for each thermocouple. The number of elements and the number of nodal points were obtained in *COMSOL*® itself through a function called “statistics.” The deviation was found using the formula $\text{Deviation} = \frac{T_{num} - T_{exp}}{T_{exp}} \cdot 100$, where T_{num} is the numerical temperature obtained in the present work using the flow measured in the laboratory by Carvalho *et al.* (2006) and T_{exp} is the experimental temperature collected in a controlled experiment (Carvalho *et al.*, 2006).

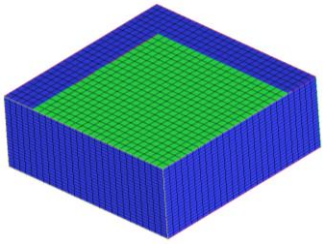

Figure 6. Cutting tool isolated.

Table 2. Study of the thermal influence of the grids on the temperature obtained from thermocouple T_1.

Tetrahedral mesh	Number of elements	Number of nodal points	Deviation [%]
Mesh 1 (*Coarser*)	897	423	4.74
Mesh 2 (*Normal*)	1396	513	4.73
Mesh 3 (*Finer*)	3390	996	4.15

Table 3. Study of the thermal influence of the grids on the temperature obtained from thermocouple T_2.

Tetrahedral mesh	Number of elements	Number of nodal points	Deviation [%]
Mesh 1 (*Coarser*)	897	423	8.78
Mesh 2 (*Normal*)	1396	513	8.78
Mesh 3 (*Finer*)	3390	996	8.17

From the tables above, it was verified that from the "*normal*" mesh the deviation found was 4.73%, being considered a satisfactory result in relation to that of the more refined mesh, which was 4.15%. Thus, in this work, the "*normal*" mesh was used to validate the numerical methodology.

Figure 7 shows the experimental thermal flux measured by Carvalho *et al.* (2006), ranging from t = 0 to 110 s. Figure 8 (a-b) below, obtained by thermocouples T_1 and T_2, presents the experimental temperature curves by Carvalho *et al.* (2006) and the numerical obtained by the present work, in which *COMSOL*® was used.

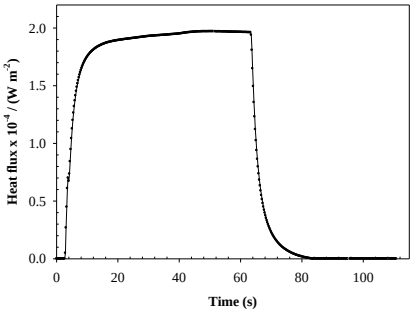

Figure 7. Experimental thermal flow (CARVALHO *et al.*, 2006).

In Figure 8(a-b) it is possible to observe that the greatest deviation found for thermocouple T_1 for the time instant of 109.67 seconds was 4.73%, and for thermocouple T_2 for the time instant of 109.67 seconds it was 8.78%. Thus, the numerical result in *COMSOL*® was satisfactory for the direct problem in which the input is known and the output is obtained.

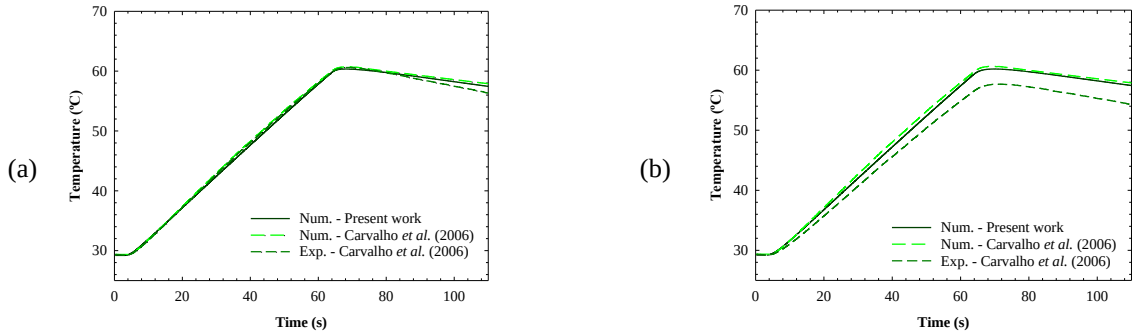

Figure 8. Thermocouples T_1 (a) and T_2 (b): comparison between the numerical temperatures calculated in this work and the experimental and numerical temperatures (CARVALHO *et al.*, 2006).

3.2 Analysis of temperature variation between thermocouples and numerical probes comparing cases with and without coating

In many dynamic situations regarding heat transfer, in a machining process for example, temperature profiles on the surface of a hard-to-reach solid or the heat flux need to be determined. Normally, these surface temperatures are obtained from temperature measurements in one or more locations where there is access to the medium. This is called the inverse problem. In a system, an inverse problem is characterized when the output is known and it is desired to estimate the input of this system.

The numerical results obtained in the present work were compared with the experimental and numerical results obtained in the work of Carvalho *et al.* (2006) and with the numerical results of Corrêa Ribeiro's work (2018), both referenced in Figs. 9a and 9b, respectively, considering the uncoated cutting tool.

Data estimated numerically by Carvalho *et al.* (2006) of the transient heat flux in the cutting tool set, shim, and tool holder through their study of the inverse problem were used in the present work as input data in the *COMSOL*® package.

Next, the numerical results of the temperatures in each thermocouple and in the analyzed numerical probes, obtained in the present work for the set of cutting tool, shim, and tool holder, are presented and analyzed. First, the case results for the uncoated assembly are presented. Figure 9a shows the temperature results for the eight numerical probes inserted via *COMSOL*® package analyzed in the same positions as the thermocouples used in the work by Carvalho *et al*. (2006). Figure 9b shows the results of the temperature values for the 11 numerical probes placed in the cutting tool and workpiece contact region, for a depth of up to 10 μm, considering the same positions of the numerical probes used in Corrêa Ribeiro's work (2018).

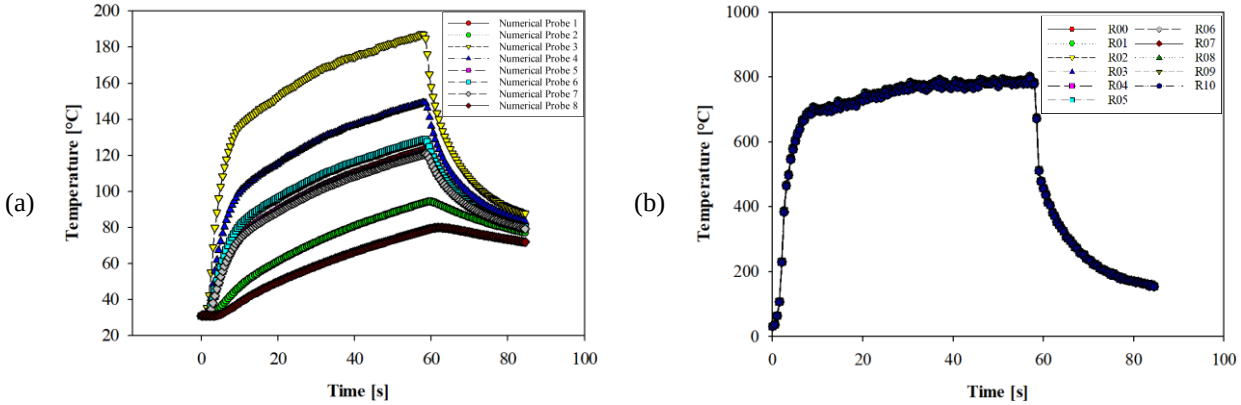

Figure 9. (a) Thermocouple temperature comparison in the uncoated case. (b) Comparison of the temperature of the 10 probes in the uncoated case.

Figures 10a and 10b present the numerical results obtained from the present work, respectively, as per the experimental and numerical results from Carvalho *et al*.'s (2006) work and numerical results from Corrêa Ribeiro's work (2018), considering the presence of the 10 μm coating.

The results of the case considering the three coating layers are shown in Figures 10a and 10b, para in which it is possible to observe that the temperature variation becomes greater due to the use of these coatings. This result is relevant, showing that coatings retain more heat on the upper face of the tool and thus prevent it from passing to the substrate and can reduce tool life.

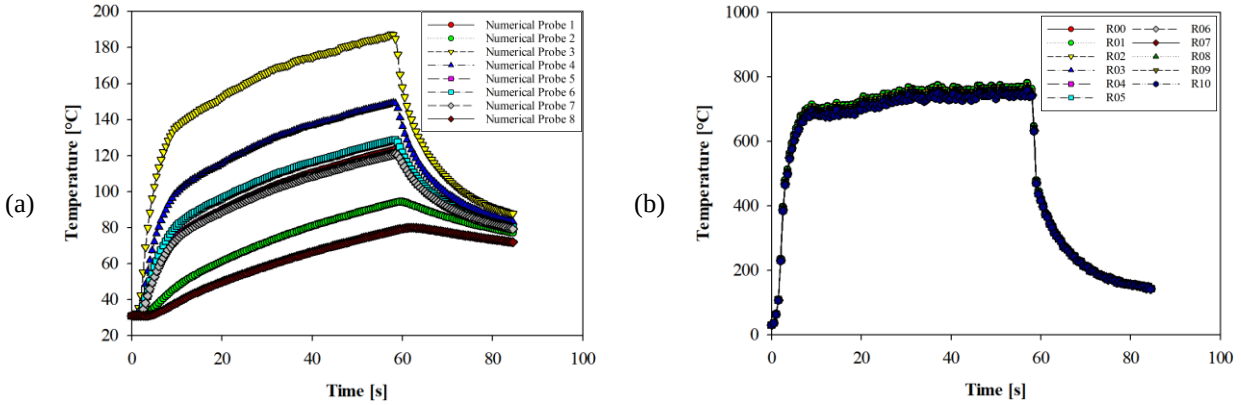

Figure 10. (a) Thermocouple temperature comparison in the case with 3 coating layers. (b) Comparison of the temperature of the 10 probes in the case with coating.

In order to make a comparison between the analyzed thermocouples, the graphs in Figures 11a, 11b, and 11c below were plotted, which respectively refer to the comparisons of the temperatures of thermocouples T_3, T_6, and T_7.

Analyzing these comparisons between the temperatures of these three thermocouples from Figures 11a, 11b, and 11c of the present work, a relevant result was not perceived as observed in the analysis of the numerical probes used inside the coating, as was performed in the work of Corrêa Ribeiro (2018). For this reason, the results of the probes started to be observed with more attention, and that is why a comparison of the values of the probes in both cases of this study was made with the values of the probes analyzed by Corrêa Ribeiro (2018).

The Figure 12 illustrates this comparison. Through this comparison, it was possible to better observe the thermal influence of the presence of coatings by this method of analysis in order to reduce the heat transfer from the contact area to the rest of the cutting tool.

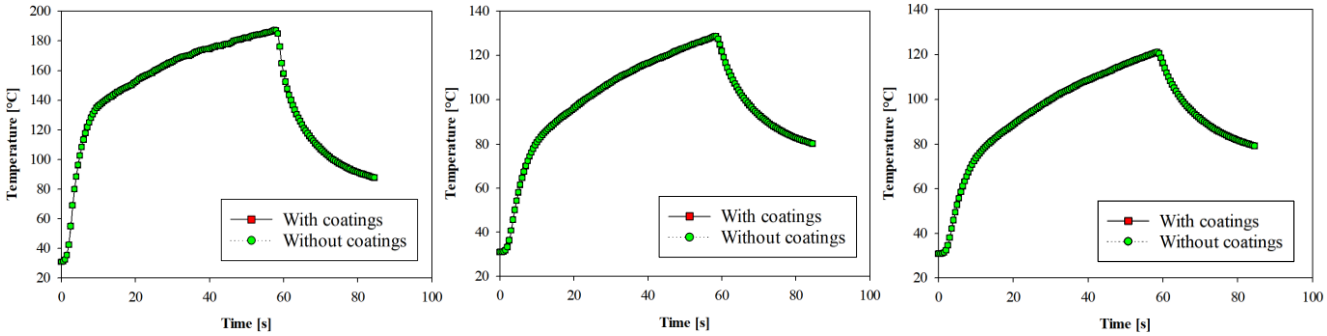

Figure 11. (a) Comparison of T_3 thermocouple temperatures. (b) Comparison of T_6 thermocouple temperatures. (c) Comparison of T_7 thermocouple temperatures.

Also, with respect to Fig. 12, it was observed that, in addition to the case considering an Alumina (Al_2O_3) coating by Corrêa Ribeiro (2018), the case of this work that considered multilayer coatings with TiN, Al_2O_3, and TiC materials presented a greater temperature variation along the numerical probes.

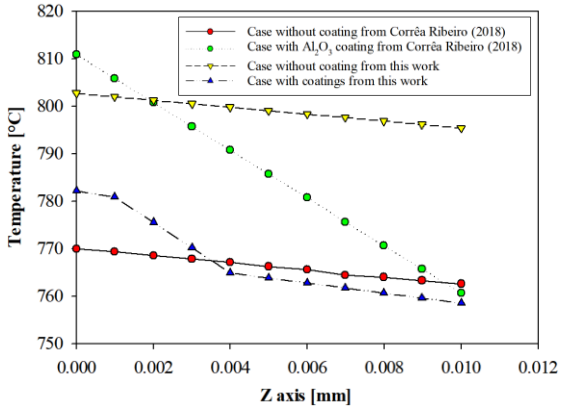

Figure 12. Comparison of coating temperatures, calculated in numerical probes of the present work, for t = 57 s, between this work and the work by Corrêa Ribeiro (2018).

According to the results obtained, it is also possible to notice a variation of approximately 23.64 °C between the R00 probe and the R10 probe (Figs. 5 and 12), in this case considering a multilayer coating of TiN, Al_2O_3, and TiC with a thickness of 10 µm.

It can also be observed that the region of the blue curve in Figure 12, which comprises the elevation of z = - 0.001 mm to z = - 0.004 mm and represents the region of the coating of Alumina Oxide (Al_2O_3) material, had a drop similar to the drop in temperature of Corrêa Ribeiro (2018), who used a coating of only Al_2O_3, represented by the green curve in the graph. In the case of Corrêa Ribeiro (2018), the temperature drop was 51.55 ºC considering only a single 10 µm-thick Al_2O_3 coating. For the case without coating, the temperature reduction in 10 µm of thickness in the cutting tool for the present work and for the work of Corrêa Ribeiro (2018) was, respectively, 7.30 ºC and 7.46 ºC.

4. CONCLUSIONS

The following conclusions can be presented in relation to the numerical results obtained for the thermal model of heat transfer in coated and uncoated cutting tools: i) The results of the present work were in agreement with the numerical results obtained by Corrêa Ribeiro (2018); ii) The studies carried out showed that for a uniform heat source with time variation, considering a surface of constant contact between the chip and the tool, the temperature in the tool is directly influenced by the coatings when the thermal properties of the coating are different from those of the substrate, even for a thin coating of 10 µm; iii) The coating layer deposited on the analyzed cemented carbide tool presented satisfactory results during the continuous cutting process. A variation of approximately 24 °C (point A) was observed between the numerical probes under analysis in the case considering the multilayer coatings (TiN, Al_2O_3, and TiC); and iv) The present analysis of heat transfer in multilayer coated carbide cutting tools revealed promising characteristics in the study of tool life, cost reduction in dry machining processes, reduction of time spent in the study of thermal influence coatings, and reduction in

the number of experiments, as well as characteristics that are also validated in other works such as Kusiak *et al*. (2005), and Marusich *et al*. (2002).

5. REFERENCES

Borelli, J.E., França, C.A., Medeiros, C.F., and Gonzaga, A., 2001. "Análise da Temperatura na Região de Contato entre a Peça e a Ferramenta", *Revista Máquinas e Metais*, pp. 114-125.

Brito, R.F., Carvalho, S.R., Lima E Silva, S.M.M., and Ferreira, J.R., 2009. "Thermal analysis in coated cutting tools", *International Communications in Heat and Mass Transfer*, Vol. 36, No. 4.

Carvalho, S.R., Lima e Silva, S.M.M., Machado, A.R., and Guimarães, G., 2006. "Temperature Determination at the Chip-Tool Interface Using an Inverse Thermal Model Considering the Tool and Tool Holder", *Journal of Materials Processing Technology*, Elsevier, Vol. 179, pp. 97-104.

Corrêa Ribeiro, C.A., 2018. *Thermal Influence Analysis of Coatings and Contact Resistance on a Turning Cutting Tool by Using COMSOL®* (in Portuguese). Doctoral Thesis, Pos-Graduate Program in Mechanical Engineering, Federal University of Itajubá, Itajubá, Brazil.

Ferreira, D.C., Magalhães, E.S., Brito, R.F., and Lima e Silva, S.M.M., 2018. "Numerical analysis of the influence of coatings on a cutting tool using *COMSOL®*", *Int. J. Adv. Manuf. Technol.*, Vol. 97, No. 1-4, pp. 1305-1314.

Ghani, J.A., Che Haron, C.H., Kasim, M.S., Sulaiman, M.A., and Tomadi, S.H., 2016. "Wear mechanism of coated and uncoated carbide cutting tool in machining process" *J. Mater. Res.*, Vol. 31, No. 13, pp. 1873-1879.

Grzesik, W., 2006. "Determination of temperature distribution in the cutting zone using hybrid analytical-FEM technique", *International Journal of Machine Tools & Manufacture*, Vol. 46, pp. 651-658.

Grzesik, W., Nieslony, P., and Bartoszuk, M., 2009. "Modeling of the Cutting Process Analytical and Simulation Methods", *Advances in Manufacturing Science and Technology*, Vol. 33, pp. 5-29.

Hao, G., and Liu, Z., 2019. "Experimental study on the formation of TCR and thermal behavior of hard machining using TiAlN coated tools", *Int. J. Heat Mass Transf.*, Vol. 140, No. 7, pp. 1-11.

Hunt, J.L., and Santhanam, A.T., 1990. "Coated Carbide Metal Cutting Tools: Development and Applications", *The Winter Annual Meeting of The American Society of Mechanical Engineers*, Vol. 25-30, pp. 139-155.

Incropera, F.P., Dewitt, D.P., Bergman, T.L., and Lavine, A., 2011. *Fundamentals of Heat and Mass Transfer*, John Wiley & Sons, Vol. 7, 1076p.

Jiang, F., Zhang, T., and Yan, L., 2016. "Estimation of Temperature-Dependent Heat Transfer Coefficients in Near-Dry Cutting", *International Journal of Advanced Manufacturing Technology*, Vol. 86, pp. 1207-1218.

Jin, D., Jingjie, Z., and Liguo, W., 2018. "Heat partition and rake face temperature in the machining of H13 steel with coated cutting tools", *Int. J. Adv. Manuf. Technol.*, Vol. 94, No. 9-12, pp. 3691-3702.

Kusiak, A, Battaglia, J.L., and Rech, J., 2005. "Tool Coatings Influence on the Heat Transfer in the Tool during Machining", *Surface & Coatings Technology*, Vol. 195, pp. 29-40.

Marusich, T.D., Brand, C.J., and Thiele, J.D., 2002. "A Methodology for Simulation of Chip Breakage in Turning Processes using an Orthogonal Finite Element Model", In *Proceedings of the Fifth CIRP International Workshop on Modeling of Machining Operation*, Vol. 5, No. 20-21, pp. 139-148.

Polozine, A., and Schaeffer, L., 2005. "Exact and Approximate Methods for Determining the Thermal Parameters of the Forging Process", *Journal of Materials Processing Technology*, Vol. 170, pp. 611-615.

Song, W., Wang, Z., Deng, J., Zhou, K., Wang, S., and Guo, Z., 2017. "Cutting temperature analysis and experiment of Ti–MoS2/Zr-coated cemented carbide tool", *Int. J. Adv. Manuf. Technol.*, Vol. 93, No. 1-4, pp. 799-809.

Tonshoff, H.K., Arendt, C., and Ben Anor, R., 2000. "Cutting of Hardened Steel", *Ann. CIRP*, Vol. 49, No. 2, pp. 547-566.

Wang, Y.M., Tian, H., Shen, X.E., Wen, L., Ouyang, J.H., Zhou, Y., Jia. D.C., and Guo, L.X., 2013. "An Elevated Temperature Infrared Emissivity Ceramic Coating Formed on 2024 Aluminum Alloy by Microarc Oxidation", *Ceramics International*, Vol. 39, pp. 2869-2875.

Yen, Y.C., Jain, A., and Altan, T., 2004. "A Finite Element Analysis of Orthogonal Machining using Different Tool Edge Geometries", *J. of Mater Process. Technol.*, Vol. 146, pp. 72-81.

Yuste, M., Galindo, R.E., Sánchez, O., Cano, D., Casasola, R., and Albella, J.M., 2010. "Correlation Between Structure and Optical Properties in Low Emissivity Coatings for Solar Thermal Collectors", *Thin Solid Films*, Vol. 518, pp. 5720-5723.

Zhang, J., and Liu, Z., 2017. "Transient and steady-state temperature distribution in monolayer-coated carbide cutting tool", *Int. J. Adv. Manuf. Technol.*, Vol. 91, No. 1-4, pp. 59-67.

Zhang, J., Liu, Z., and Du, J., 2017. "Prediction of cutting temperature distributions on rake face of coated cutting tools", *Int. J. Adv. Manuf. Technol.*, Vol. 91, No. 1-4, pp. 49-57.

6. RESPONSIBILITY NOTICE

The authors are the only responsible for the printed material included in this paper.